Accepted Manuscript

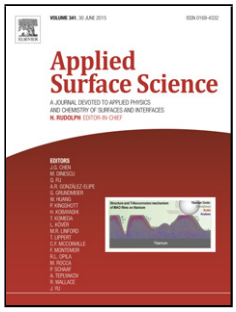

Title: Rhodium clustering process on defective (8,0) SWCNT: Analysis of chemical and physical properties using density functional theory

Authors: Ruben E. Ambrusi, C. Romina Luna, Mario G. Sandoval, Pablo Bechthold, M. Estela Pronsato, Alfredo Juan

PII: S0169-4332(17)32060-3
DOI: http://dx.doi.org/doi:10.1016/j.apsusc.2017.07.070
Reference: APSUSC 36604

To appear in: *APSUSC*

Received date: 6-4-2017
Revised date: 3-7-2017
Accepted date: 9-7-2017

Please cite this article as: Ruben E.Ambrusi, C.Romina Luna, Mario G.Sandoval, Pablo Bechthold, M.Estela Pronsato, Alfredo Juan, Rhodium clustering process on defective (8,0) SWCNT: Analysis of chemical and physical properties using density functional theory, Applied Surface Sciencehttp://dx.doi.org/10.1016/j.apsusc.2017.07.070

This is a PDF file of an unedited manuscript that has been accepted for publication. As a service to our customers we are providing this early version of the manuscript. The manuscript will undergo copyediting, typesetting, and review of the resulting proof before it is published in its final form. Please note that during the production process errors may be discovered which could affect the content, and all legal disclaimers that apply to the journal pertain.

ACCEPTED MANUSCRIPT

Rhodium Clustering Process on Defective (8,0) SWCNT: Analysis of Chemical and Physical Properties Using Density Functional Theory

Ruben E. Ambrusi[a], C. Romina Luna[a], Mario G. Sandoval[a], Pablo Bechthold[a], M. Estela Pronsato[a], Alfredo Juan[a]*

[a] Departamento de Física and Instituto de Física del Sur (UNS-CONICET) Av. Alem 1253, 8000, Bahía Blanca, Argentina

***Corresponding Author:**

Dr. Alfredo Juan
Telephone:+54 0291 4595101
E-mail address: cajuan@uns.edu.ar
Postal address: Departamento de Física and Instituto de Física del Sur (UNS-CONICET), Av. Alem 1253, 8000, Bahía Blanca, Argentina

ACCEPTED MANUSCRIPT

Graphical abstarct

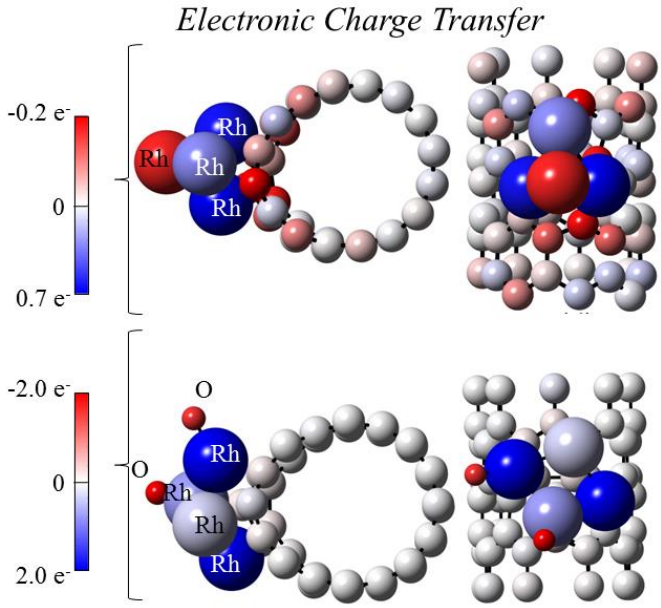

Highlights

- Rh3 and Rh4 clusters prefer to be adsorbed on oxygenated vacancy.
- Rh adsorption induces a magnetic moment.
- Rh atom and Rh2 dimer bonded to the defective SWCNT, show a semiconductor behavior.
- Rh3 and Rh4 show a metallic behavior.

Abstract

The Spin-polarized density functional theory is used to study the effect of a single vacancy in a (8,0) single-walled carbon nanotube (SWCNT) on the Rh clustering process. The vacancy is considered oxygenated and non-oxygenated and, in each case, different Rh_n cluster sizes (n =1- 4) are taken into account. For the analysis of these systems some physical and chemical properties are calculated, such as binding energy (E_b), work function (WF), magnetic moment, charge transfer, bond length, band gap (E_g), and density of state (DOS). From this analysis it can be concluded that: a single Rh atom and Rh_2 dimer are adsorbed on vacancy without oxygen, whereas Rh_3 and Rh_4 clusters prefer to be adsorbed on oxygenated vacancy. In all cases, Rh adsorption induces a magnetic moment. When the Rh atom and Rh_2 dimer are bonded to the

ACCEPTED MANUSCRIPT

defective SWCNT, it has been found that they show a semiconductor behavior that could be interesting to use in the spintronic area. In the case of Rh_3 and Rh_4 clusters our results show a metallic behavior suggesting that these systems are good candidates for nanotube contact.

Keywords: CNT, DFT, VACANCY, ADSORPTION

1. Introduction

Carbon nanotubes (CNTs) are one of the most widely explored one-dimensional nanostructures for the scientific community. These structures show particular mechanical and electronic properties due to their curvature. CNTs have been used by many laboratories to build nano-device prototypes such as metallic wires, field-effect transistors (FET), gas sensors, and hydrogen storage, among others [1-10].

CNTs have different types of defects, like many other materials, such as vacancies, meta-stable atoms, pentagons, heptagons, Stone-Wales defects (SW or a pair of 5–7 rings), wall discontinuities, and heterogeneous atoms [11-15]. These defects play an important role in CNTs: they can modify CNTs chemical and physical properties [16]. In particular, defective single-walled carbon nanotubes (SWCNTs) present interesting electric properties that open new potential applications in nano-devices [17]. Vacancy defects are sites that are more chemically reactive than other SWCNT sites. For this reason, the literature reports that these types of defects interact with oxygen atoms and, therefore, there are some oxidized carbon atoms in the defect sites [18-21].

The introduction of a carbon vacancy into a small diameter SWCNT increases the adsorption energy of the transition metal (TM) cluster in comparison to pristine nanotube or to graphite sheet surfaces [22-27]. On the other hand, it is well known that the addition of TM to a CNT improves hydrogen adsorption as well as electrical contact

ACCEPTED MANUSCRIPT

[25-29]. The TMs that have been investigated most widely as possible candidates are Rh, Ti, Pd, Al, and Pt [24, 30-33]. Recently, it has been reported that Rhodium shows a quite different surface behavior on SWCNTs compared to Ti interacting less strongly with oxygen [24,33]. Suarez-Martinez et al. have applied X-ray photoelectron spectroscopy combined with high-resolution transmission electron microscopy in order to investigate the formation of the interface between Rh and (8,0) SWCNT [24]. Their results suggest that Rh atoms nucleate forming small clusters -tetrahedra Rh_4- at the oxygenated defect sites of SWCNT; therefore, the authors propose Rh as a good candidate for nanotube contacts.

Several studies that consider the interaction of transition metals and carbon nanotubes can be found. For example, the adsorption of Ni on vacancy modified (8,0) single-walled carbon nanotubes strongly changes the sensitivity to SO_2 when compared to a pristine tube [34]. In a related system, a study of Ti-adatoms adsorbed on the double-vacancy defected graphene (DG) indicates that the adsorption energy of Ti atoms on the defective graphene is higher than the one on the perfect sheet [35]. For these reasons, understanding the interaction between Rh and the SWCNT surface is fundamental in applications such as nanotube contact, gas sensor, hydrogen storage, field-effect transistor (FET) and spintronic area.

In this work, we have studied the changes in physical and chemical properties of Rh-defective (8,0) SWCNT using density functional theory (DFT) calculations. Vacancy defect type is considered in (8,0) SWCNT and in its oxygenated state. In both cases, the Rh nucleation, from a single Rh atom to a Rh_4 cluster, is studied. The present calculations show that the Rh adsorption on defective SWCNT is significantly improved by the presence of oxygen on the SWCNT surface. The case of multiple vacancies is not considered because previous studies indicated that Rh adsorption is thermodynamically

ACCEPTED MANUSCRIPT

more stable on single vacancies [36]. The obtained results, report for the first time the induced magnetic moment and changes in the work function and band gap for the adsorbed Rh_n cluster on defective (8,0) SWCNT.

2. Computational Model

All calculations were performed under the framework of first principles DFT implemented through the Vienna Ab initio Simulation Package (VASP) code [37,38]. For the exchange-correlation functional the generalized gradient approximation (GGA) and the Perdew, Burke, and Ernzerhof (PBE) function were considered [39,40]. The kinetic energy cutoff of 700 eV was found to converge the total energy within 10^{-4} meV. In addition, Brillouin zone sampling was performed using the *k*-point generation scheme of Monkhorst and Pack (the Γ-point was included) [41]. For relaxing calculations, the Brillouin zone was sampled by 1 × 5 × 1 and the convergence criteria was set to be 10^{-3} eV/Å on each atom. In the case of dispersion forces the DFT-D2 Grimme method was considered such as are suggested in the Ref. [36,42], where Van der Waals interactions are described via a simple pair-wise force field, optimized for several popular DFT functionals [43]. The minima of the total energy were found using a conjugate gradient (CG) algorithm. Finally, eleven k-points were used for sampling the one dimensional Brillouin zone in order to compute adsorption energies, magnetic moment, total density of states (TDOS) curves, projected density of states (PDOS) curves, Bader´s charges [44], and electrostatic potential.

The (8,0) SWCNT is considered and its geometrical structure is generated in a periodic supercell of 20 Å x 8.53 Å x 20 Å. The nanotube is modeled using 64 C atoms, that is to say two (8,0) SWCNT unit cells, thus ensuring no interaction among periodic

ACCEPTED MANUSCRIPT

images. The vacancy defect in the (8,0) SWCNT is simulated by removing a carbon atom.

The formation energy (E_{form}) for a single carbon vacancy is equivalent to the energy required to break the interatomic bonds around one atom [45]. The E_{form} is calculated using the following equation:

$$E_{form} = E_T(\text{SWCNT+Vac}) + \mu(\text{C}) - E_T(\text{SWCNT}) \quad (1)$$

where E_T(SWCNT+Vac) is the total energy for the nanotube with a single vacancy, μ(C) is the chemical potential for a C-atom calculated as the energy per atom for the corresponding pristine SWCNT and E_T(SWCNT) is the total energy for the pristine SWCNT [25]. On the other hand, the adsorption energy E_{ads} of an O_2 molecule on SWCNT+Vac is computed as:

$$E_{ads} = E_T(\text{SWCNT+O}_2\text{ Vac}) - E_T(\text{SWCNT+Vac}) - E(\text{O}_2) \quad (2)$$

where E_T(SWCNT+O_2 Vac) and E(O_2) are the total energies of SWCNT+Vac with the adsorbed O_2 and the isolated O_2 molecule respectively. Finally, for defective SWCNT the binding energy (E_b) of an Rh_n cluster on SWCNT is defined as:

$$E_b = E_T(\text{SWCNT+Vac}) + E(\text{Rh}_n) - E_T(\text{SWCNT+Vac+Rh}_n) \quad (3)$$

where E(Rh_n) is the total energy of the isolated Rh cluster that contains n Rh atoms and E_T(SWCNT+Vac+Rh_n) corresponds to the total energy of defective SWCNT with the same Rh_n cluster bonded. Vacancy can be oxygenated or not.

3. Results and Discussion

3.1 Isolated Rh Clusters

ACCEPTED MANUSCRIPT

There are several different theoretical research approaches to Rh_n clusters formation and their associated properties [46-51]. Based on this information, we only used the most stable geometric structure for each cluster size. Optimized geometry, binding energy per atom (E_b/atom), magnetic moment (μ), bond lengths, and angles corresponding to Rh_n (n = 1-4) ground states are reported in Table 1.

- Table 1 here -

In Table 1 it can be seen that the E_b/atom increases when the number of Rh cluster atoms grows. In addition, we found that the magnetic character and the magnetic moment vary with Rh_n size. Rh_2 and Rh_3 clusters have high magnetic moments and are ferromagnetic. Whereas the Rh_4 cluster has a nonmagnetic ground state. Detailed experimental and theoretical studies about small Rh clusters can be found in the literature [46-51].

3.2 Defective SWCNT

After relaxation, we obtained two stable vacancy geometries that are shown in Figure 1-a and -b. The ground state is a perpendicular configuration where the new C-C bonds are between 1.42 Å and 1.82 Å. The parallel geometry is a meta-stable state with C-C bond lengths in the range of 1.34 Å –1.74 Å. Similar results are reported in the literature [52-54]. In addition, there is a slight change in the curvature in defective SWCNT compared to pristine SWCNT. Without vacancy, the nanotube has a diameter of 6.37 Å. In the case of perpendicular (parallel) geometry the diameter elongation and contraction are 8% (7%) and 6% (2%), respect to pristine SWCNT, respectively.

- Figure 1 here -

ACCEPTED MANUSCRIPT

Figure 1-c and -d show the DOS curves for a SWCNT with perpendicular and parallel vacancy configuration respectively. It can be noted that the electronic behavior is very different in both configurations. From Figure 1-c it can be seen that the DOS curves -spin up and spin down contributions- are symmetric for the perpendicular configuration; whereas in the case of the parallel vacancy orientation the DOS curves are asymmetric around 1 eV below the Fermi level (see Figure 1 -d). Table 2 presents the band gap (E_g), magnetic moment (μ), work function (WF) and E_{form} for the same structures. The perpendicular vacancy configuration does not have a magnetic moment and its electronic structure behaves like a semiconductor with a band gap of 0.48 eV. In a previous work we have found that the pristine (8,0) SWCNT is a semiconductor with a relatively large band gap (E_g = 0.58 eV) and without magnetic moment [30]. Moreover, the Fermi level of pristine (8,0) SWCNT is located near to the valence band (VB); then its behavior resembles a p-type semiconductor. Therefore, the band gap obtained for the perpendicular configuration is lower than that of the pristine SWCNT -around 21%- and it has also a p-type semiconductor behavior with no magnetic moment, whereas the parallel configuration presents a metallic behavior and a magnetic moment of 1.0 μ_B.

- Table 2 here -

The work function is computed as the difference between vacuum and Fermi levels. The WF for a pristine SWCNT is 4.39 eV [30]. The presence of a vacancy increases the WF about 11% (7%) for perpendicular (parallel) configuration. The formation energies for a single vacancy are 5.88 and 6.65 eV for the perpendicular and parallel configuration respectively. The energies calculated Ma *et al.* fall in the same range [53]. Our results indicate that the formation of a vacancy with perpendicular

ACCEPTED MANUSCRIPT

configuration is energetically more favorable. For this reason, only the results for the perpendicular configuration of a single vacancy on (8,0) SWCNT are presented below.

The effect of removing one C atom leads to a redistribution of charge on SWCNT around the defect, as it can be seen in Figure 2. In the case of the most stable vacancy configuration it is noted that C atoms named C1, C2 and C3 are negatively charged, and each one gains 0.09 e^-, 0.04 e^-, and 0.09 e^- respectively. The other C atoms -that form the defect- lose charge 0.01 e^- to 0.05 e^-. The remaining atoms practically do not change their charge compared to the pristine nanotube [30]. The adsorption of O_2 molecules in the SWCNT with vacancy will be discussed in detail in the following section. It can be anticipated that carbon atoms with a negative charge are expected to be the ones interacting with the O_2 molecules. In principle this is not strange, based on the fact that O atoms can achieve the already known and more stable electronic configuration of the subsequent noble gas, accepting electrons.

- Figure 2 here -

3.3 Oxygenated Vacancy

Several O_2 molecule disposal and orientation were tested in order to obtain the most stable configuration. Near the vacancy, we found the molecule adsorbed and dissociated (see Figure 3). There is an elongation and a contraction of the SWCNT diameter compared to the pristine nanotube, 13.2% (6.37 Å to 7.21 Å) and 6.6% (from 6.37 Å to 5.95 Å) respectively. It can also be seen in Figure 3, that the O atoms are adsorbed on sites near C1 and C3 atoms, after O_2 adsorption.

- Figure 3 here -

ACCEPTED MANUSCRIPT

The oxidation of the defective SWCNT surface involves the bonding of a pair of O atoms in the neighborhood of a single C vacancy, resulting in C-O-C ether and C=O ketone functional groups, as it was proposed in the initial stages of oxidation on graphitic surfaces [55]. The bond lengths, angles and geometry of ketone and ether groups are listed in Table 3.

- Table 3 here -

The adsorption energy of the O_2 molecule on defective SWCNT is -5.23 eV with zero magnetic moment. Suarez-Martinez *et al.* modeled the O_2 adsorption on a single carbon vacancy on graphene and found the molecule also dissociated on the surface [24]. The computed band gap is 0.24 eV. There is an E_g reduction of 49% with respect to that SWCNT containing a single vacancy (0.48 eV) and 58% with respect to a pristine nanotube (0.58 eV). In addition, the WF increases 3.5 % with respect to defective SWCNT (4.89 eV to 5.06 eV).

Figure 4 shows the density of states for defective SWCNT with O_2 adsorbed. In Figure 4-a it can be noted, that the Fermi level is closer to valence band (VB, E_F-E_{VB}=0.04 eV) than to conduction band (CB, E_{CB}-E_F=0.20 eV), then the SWCNT with a single oxygenated vacancy is a p-type semiconductor. The PDOS curves on adsorbed O atoms (see Figure 4-b), show that *p*-states shift to lower energies near the Fermi level and spread over a higher energy range (approximately -2.5 to -1 eV) compared to the O atom *p*-states of the isolated molecule. In addition, the *p*-states of C atoms and adsorbed O atoms have the same energy range in the PDOS curves, concluding that an hybridization between *p*-states of C and O atoms is present (see Figure 4-b and 4-c).

- Figure 4 here -

ACCEPTED MANUSCRIPT

Figure 5 shows the charge transfer when the O_2 molecule is adsorbed on defective (8,0) SWCNT. The O atoms are electron acceptors and the charge transfer from C to O is significant. This is in agreement with their higher E_{ads}. The most important charge transfer occurs among the atoms in each functional group, C-O-C and C=O. In Figure 5, C10, O1 and C1 atoms correspond to the ether group, while the O2 and C3 atoms form the ketone group. The O1 atom gains 0.83 e^-, whereas the C10 and C1 atoms lose 0.37 e^- and 0.35 e^- respectively. Finally, in the ketone group the O2 atom becomes negatively charged -with a gain of 1.8 e^--, while the C3 atom loses 1.8 e^-. The charge transfer from SWCNT to O atoms explains the change in the band gap and WF.

- Figure 5 here -

3.4 Rh Clusters on Defective SWCNT

In this section, we studied Rh_n (n = 1 to 4) adsorption on defective SWCNT with and without O_2 adsorbed on the C vacancy. Figure 6 shows the optimized structures after Rh_n is adsorbed in each case. Following the Rh adsorption, the SWCNT diameter increases in the direction of cluster adsorption, whereas in the perpendicular direction the diameter experiments a contraction (see Figure 6). This behavior is more significant in the case of an oxygenated vacancy. If we compare the diameter elongation between oxygenated and non-oxygenated vacancy, the main difference appears in Rh_2 (~ 5.4%) and the less significant one in Rh_4 (~ 1.7%). Therefore, because of the SWCNT curvature modifications due to the Rh and O atoms presence, electronic changes are expected.

- Figure 6 here -

ACCEPTED MANUSCRIPT

- Table 4 here -

Table 4 lists the C-C, Rh-C, Rh-Rh, O-C and O-Rh bond lengths. It can be noted that the geometry of a Rh cluster has practically not modified its form and bond lengths when is adsorbed on the clean vacancy (compare Table 1 and Table 4). This behavior could be attributed to the high cohesive energy of Rh as the cluster is formed (see Table 1). The C-C bonds become shorter when a single Rh atom and the Rh_2 dimer are adsorbed on the surface when oxygen atoms are present; whereas the opposite occurs for the Rh_3 and Rh_4 clusters. In addition, based on the d_{Rh-C} and d_{Rh-Rh} bond distances, the Rh-SWCNT and Rh-Rh cohesive interactions become weaker on the oxygenated vacancy. Regarding the C-O bonds, they are elongated after Rh_n adsorption. For atomic Rh adsorbed on the oxygenated vacancy, Rh atom is bonded to both oxygen atoms and the ether group practically suffers no distortion at all. With the addition of more Rh atoms, covering the oxygenated vacancy zone on defective SWCNT, a weakening in C-O bonds (higher d_{O-C}) and the formation of Rh-O bonds, is observed. The ketone group is the less affected. The Rh-O bond length for the Rh_4 cluster is 1.75 Å, similar to the length obtained by DFT calculations on a single isolated Rh atom [46]. Suarez-Martinez *et al.*, conclude from XPS and TEM analysis that Rh-O bonds are developed at the expense of C-O bonds at the Rh-CNT interface [24].

The binding energy (E_b), magnetic moment (μ), and work function (WF) obtained for each case are presented in Table 5. In a previous work where the Rh single atom adsorption on the pristine (8,0) SWCNT was studied, we found that the binding energy value is 2.67 eV [30]. It can be noted that the oxygenated and non-oxygenated vacancy incorporation improves the adsorption of one Rh atom (7.56 eV and 5.12 eV respectively). The binding energy for the adsorption of a single atom and a dimer of Rh

ACCEPTED MANUSCRIPT

is smaller when the vacancy is oxygenated (see Table 5). In the case of a single Rh atom the E_b decreases 2.44 eV (7.56 eV to 5.12 eV) and in the case of Rh_2 the decrease is 1.39 eV (6.31 eV to 4.92 eV). This behavior could be attributed to the passivation of the active dangling bond by the effect of oxygen [56]. The Rh_3 and Rh_4 clusters energetically prefer to be adsorbed on the oxygenated vacancy. The E_b on the oxygenated defect is 1.03 eV and 0.96 eV higher than in the clean defect for Rh_3 and Rh_4, respectively.

- Table 5 here -

Considering the variation of E_b with the number of Rh atoms on the SWCNT without oxygen, it decreases when more Rh atoms are added. This tendency is not clear in the case of SWCNT+O_2Vac. Not only Rh-C, but also Rh-O and O-C interactions are present and these interactions are different depending on the size of the cluster.

Another aspect is that the Rh bonding induces a magnetic moment on the defective SWCNT, with and without oxygen (see Table 5). This happens when a nonmagnetic material, i.e. the defective SWCNT, is bonded with a magnetic system (Rh cluster). These μ values are slightly lower than those obtained for isolated Rh_n clusters when n = 1, 2, and 3 (compare with data in Table 1). In addition, contrasting the magnetic moments between the clean and oxygenated vacancy systems, no significant changes are found, except when the Rh_3 cluster is adsorbed. In particular, the Rh_4 isolated cluster does not present a magnetic moment (see Table 1). Nevertheless, when this cluster is adsorbed on a defective SWCNT, a magnetic moment is induced (~ 2 μ_B).

Concerning the WF, there is a variation after Rh_n adsorption, the same is reduced with respect to the clean (4.89 eV) and oxygenated vacancy system (5.06 eV). In

ACCEPTED MANUSCRIPT

particular, in the case of the vacancy without oxygen, the main reduction in WF occurs for the Rh_3 cluster when compared to the WF of a defective SWCNT (4.89 eV to 4.16 eV). In the case of the Rh_4 bonded to SWCNT+ O_2Vac, the WF has a slight change of about 0.4% (5.06 eV to 5.09 eV). Sathe et al. have reported that the functionalization of CNT using Rh nano-clusters presumably decreases the local work function of field emitters, enabling an increase in the density of states (DOS) near the Fermi level of the CNTs surface due to the co-operative nature of electronic interactions with Rh [55].

Figure 7 shows the density of states for the Rh_n adsorbed on defective SWCNT with and without O_2. The main contribution to the total DOS curve is due to the *p*-sates of carbon and oxygen atoms, and the *d*-states of Rh atoms. According to Sathe et al., there is an increase of states due to Rh atoms near to the Fermi level, i.e. Rh atoms induce novel states within the band gap of defective SWCNT [57]. The main contribution of the *d*-state of Rh atoms to the total DOS curve is around Fermi level (between -2.5 eV and 2.5 eV) in all cases. Moreover, it can be noted that the interaction between Rh and C atoms decreases when the size of the Rh cluster increases.

- Figure 7 here -

Total DOS and PDOS curves for the adsorption of a single Rh atom on the defective SWCNT with and without oxygen are shown in Figure 7-a and -b respectively. The spin up and spin down contributions for the clean vacancy when a Rh atom is adsorbed show a different behavior (see Figure 7-a). The spin up contribution has a conductor behavior; whereas the spin down contribution shows a n-type semiconductor behavior with a band gap of 0.29 eV. When oxygen is incorporated to the defect, the Rh SWCNT+O_2Vac system presents a metallic behavior (see Figure 7-b). This fact is due to the hybridization between the *p*-state of O and the *d*-state of Rh

ACCEPTED MANUSCRIPT

atoms. In addition, it can be seen that between -3 eV and -2 eV there is a strong interaction of Rh-O.

Figure 7-c shows the total DOS and PDOS when the Rh_2 dimer is adsorbed on defective SWCNT without O atoms. The total DOS curve for the spin up contribution presents a semiconductor behavior and the band gap obtained is 0.32 eV. The spin down contribution has a metallic behavior. These effects are due to the *d*-states of Rh atoms. When the vacancy is oxygenated, both contributions of the DOS curve -spin up and spin down- have a metallic behavior (see Figure 7-d).

The adsorption of Rh_3 and Rh_4 on defective SWCNT have a magnetic metallic behavior, regardless of the fact of the vacancy being oxygenated or not (see Figure 7 –e to-h). In all cases, the total DOS curves are asymmetrical around the Fermi level. In Figure 7 -e it is noted that the major Rh-C interaction occurs between -4 eV and 1 eV. This hybridization decreases when there are oxygen atoms (see Figure 7 -f) due to a strong Rh-O interaction, as it was mentioned in the previous paragraphs. The hybridization occurs around the Fermi level, for this reason the system has a metallic behavior. The Rh_4 cluster adsorption on clean vacancy shows an important peak increase on the *d*-states of Rh atoms at -0.5 eV and at the Fermi level (see Figure 7-g). The presence of O atoms, contributes to a more intense Rh-O hybridization when it is compared with the other systems (see Figure 7-h). In the same figure, an extensive overlap between the Rh *d*-states and the O *p*-states can also be seen. In addition, there is an interaction between *d*-states of Rh and *p*-states of C atoms.

Finally, we studied the charge transfer among the atoms of the different systems. Figure 8 shows the charge transfer among the Rh, SWCNT and O atoms. As it can be noted, the electronic distribution is very sensitive to the presence of O in the system. The Rh atom acts as an electron donor; its charge is transferred to the SWCNT carbon

ACCEPTED MANUSCRIPT

atoms located below the adatom. Nevertheless, the main transfer is from the Rh to the O atoms. In the case of the Rh_2 and Rh_4 adsorbed on SWCNT+Vac, some electrons are also shared with Rh atoms. These results are consistent with the obtained DOS curves, which show a high density of states around the Fermi level. This can be related with accepted or donated electrons, corresponding to C, O and Rh atoms as shown in PDOS curves (Figure 7). For non-oxygenated vacancy, after the Rh adsorption the unoccupied *p*-states located close to the Fermi level tend to decrease and shift to lower energies, compared to the same states before the Rh adsorption. This indicates that the electrons are transferred from Rh to C atoms (see Figure 8-a to -d). Furthermore, when the vacancy is oxygenated, the O atoms PDOS main states are concentrated in the valence band and few states in the conduction band, showing that O atoms behave as electron acceptors. This result agrees with Bader analysis (see Figure 8-e to -h).

- Figures 8 here -

Conclusions

The Rh cluster adsorption on defective SWCNT, with -clean or oxygenated-vacancy leads to changes in the geometric and electronic structures at the metal-SWCNT contact. In all cases studied, the Rh adsorption reduces the WF and induces an important magnetic moment.

In the case of a single Rh atom and Rh dimer, the adsorption is energetically favorable when the vacancy on SWCNT is non-oxygenated. Spin up and spin down contributions have different behaviors -semiconductor or metal behavior. For this reason, we believe that the use of these systems is relevant in the spintronic area.

ACCEPTED MANUSCRIPT

Calculations suggest that the Rh prefers to be configured as a 3D cluster (Rh_4) at the non-oxygenated vacancy, whereas at the oxygenated vacancy the Rh atoms form a sort of distorted 2D configuration over the defect. The Rh and O atoms bonded to the defective SWCNT induce a considerable magnetic moment and the system has a magnetic metallic behavior. Similar results are obtained in the case of the Rh_3 cluster. This result could be used in SWCNT-Rh electrical contact.

Acknowledgements

The authors acknowledge the financial support given by SGCyT-UNS, CONICET (PIP 2014-2016: GI11220130100436CO and PICT-2014-1351). All authors are members of CONICET**.** We thank useful discussion with Prof. P. Jasen and the valuable comments from the reviewers and the editor.

References

[1]M.P. Ababtram, F. Léonard, Physics of carbon nanotube electronic devices, Rep. Prog. Phys. 69 (2006) 507-561.

[2]S. Dresselhaus, G. Dresselhaus, P. Avouris, Carbon Nanotubes, synthesis, structure, properties and applications, Springer, Berlin, 2001.

[3] J. Li, E. Croiset, L. Ricardez-Sandoval, Carbon nanotube growth: First-principles-based kinetic Monte Carlo model, J. Catal. 326 (2015) 15-25.

[4] N. Geblinger, A. Ismach, E. Joselevich, Self-organized nanotube serpentines, Nat. Nanotechnol. 3 (2008) 195-200.

[5] A. Fonseca, K. Hernadi, P. Piedigrosso, J. Colomer, K. Mukhopadhyay, R. Doome, S. Lazarescu, L.P. Biro, P. Lambin, P.A. Thiry, D. Bernaerts, J.B. Nagy, Synthesis of single- and multi-wall carbon nanotubes over supported catalysts, Appl. Phys. A 67 (1998) 11-22.

[6]Y. Yao, Q. Li, J.I. Zhang, R.A. Liu, L. Jiao, Y.T. Zhu, Z. Liu, Temperature-mediated growth of intramolecular single-walled carbon-nanotube intramolecular junctions, Nat. Mater. 6 (2007) 283-286.

ACCEPTED MANUSCRIPT

[7]C. Cantalini, L. Valentini, I. Armentano, J.M. Kenny, L. Lozzi, S. Santucci, Carbon nanotubes as new materials for gas sensing applications, J. Eur. Ceram. Soc. 24 (2004) 1405-1408.

[8]Y. Cheng, O. Zhou, Electron field emission from carbon nanotubes, C.R. Phys. 4 (2003) 1021-1033.

[9]H. Yu, J. Zheng, P. Guo, Z. Zhang, Spin transport properties of a carbon nanotube/zigzag graphene nanoribbon junction : a first principles investigation, Appl. Phys. A 117 (2014) 21175-21181.

[10]S.M. Lee, K.S. Park, Y.G. Choi, S.C. Yu, N. Kim, T. Frauenheim, Y.H. Lee, Hydrogen adsorption and storage in carbon nanotubes, Semicond. Sci. Technol. 113 (2000) 209-216.

[11]F. Banhart, Irradiation effects in carbon nanostructures, Rep. Prog. Phys. 62 (1999) 1181–1221.

[12]S. Lijima, T. Ichihashi, Y. Ando, Pentagons, heptagons and negative curvature in graphite microtubule growth, Nature 356 (1992) 776–778.

[13]O. Zhou, R.M. Fleming, D.W. Murphy, C.H. Chen, R.C. Haddon, A.P. Ramirez, et al., Defects in carbon nanostructures, Science 263 (1994) 1744–1747.

[14]J.C. Charlier, Defects in carbon nanotubes, Accounts Chem. Res. 35 (2002) 1063–1069.

[15]E. Saether, Transverse mechanical properties of carbon nanotube crystals—part II: sensitivity to lattice distortions, Compos. Sci. Technol. 63 (2003) 1551–1559.

[16]A. Robinson, E.S. Snow, S.C. Badescu, T.L. Reinecke, F.K. Perkins, Role of defects in single-walled carbon nanotube chemical sensors, Nano Lett. 6 (2006) 1747–1751.

[17]L.G. Tien, C.H. Tsai, F.Y. Li, M.H. Lee, Band-gap modification of defective carbon nanotubes under a transverse electric field, Phys. Rev. B 72 (2005) 245417.

[18]D.B. Mawhinney, V. Naumenko, A. Kuznetsova, J.T. Yates, J. Liu, R.E. Smalley, Surface defect site density on single walled carbon nanotubes by titration, Chem. Phys. Lett. 324 (2000) 213–216.

[19]Q. Zhou, X. Yang, Z. Fu, C. Wang, L. Yuan, H. Zhang, et al., DFT study of oxygen adsorption on vacancy and stone–wales defected single-walled carbon nanotubes with Cr-doped, Physica E 65 (2015) 77–83.

[20]X. Correig, A. Felten, C. Bittencourt, G. Van Lier, J.C. Charlier, J.J. Pireaux, Oxygen functionalization of MWNT and their use as gas sensitive thick-film layers, Sensor Actuat. B-Chem. 113 (2006) 36–46.

ACCEPTED MANUSCRIPT

[21] J.M. Carlsson, F. Hanke, S. Linic, M. Scheffler, Two-step mechanism for low-temperature oxidation of vacancies in graphene, Phys. Rev. Lett. 102 (2009) 166104.

[22] D. Barraza-Jimenez, D.H. Galvan, A. Posada-Amarillas, M.A. Flores-Hidalgo, D. Glossman-Mitnik, M. Jose-Yacaman, Computational study of Au_4 cluster on a carbon nanotube with and without defects using QM/MM methodology, J. Mol. Model 18 (2012) 4885–4891.

[23] I. Suarez-Martinez, A. Felten, J.J. Pireaux, C. Bittencourt, C.P. Ewels, Transition metal deposition on graphene and carbon nanotube, J. Nanosci. Nanotech. 9 (2009) 6171–6175.

[24] I. Suarez-Martinez, C.P. Ewels, X. Ke, G. Van Tendeloo, S. Thiess, W. Drube, et al., Study of the Interface between Rhodium and carbon nanotubes. ACS Nano 4 (2010) 1680–1686.

[25] H.L. Zhuang, G.P. Zheng, A.K. Soh, Interactions between transition metals and defective carbon nanotubes, Comp. Mater. Sci. 43 (2008) 823-828.

[26] P. Modak, B. Chakraborty, S. Banerjee, Study on the electronic structure and hydrogen adsorption by transition metal decorated single wall carbon nanotubes, J. Phys. Condens. Matter 24 (2012)185505.

[27] M.M. Larijani, S. Safa, Increase of hydrogen storage capacity of CNTs by using transitions metal, metal oxide-CNT nanocomposites, Acta Phys. Pol. A 126 (2014) 732-735.

[28] M. Mananghaya, E. Rodulfo, G.N. Santos, A.R. Villagracia, A.N. Ladines, Theoretical investigation on single-wall carbon nanotubes doped with nitrogen, pyridine-like nitrogen defects, and transition metal atoms, J. Nanomater. 104891 (2012) 1-14.

[29] H. Valencia, A. Giland, G. Frapper, Trends in the hydrogen activation and storage by adsorbed 3d transition metal atoms onto graphene and nanotube surfaces: A DFT study and molecular orbital analysis, J. Phys. Chem. C 119 (2015) 5506–5522.

[30] C.R. Luna, V. Verdinelli, E. German, H. Seitz, C. Pistonesi, M. Volpe, P. Jasen, Hydrogen adsorption and associated electronic and magnetic properties of Rh-decorated (8,0) carbon nanotubes using density functional theory, J. Phys. Chem. C 119 (2015) 13238–13247.

[31] P.F. Yang, J.M. Hu, B. Teng, F.M. Wu, S.Y. Jiang, Density functional theory study of rhodium adsorption on single-wall carbon nanotubes, Acta Phys. Sin. 58 (2009) 3331-3337.

[32] W. Kim, A. Javey, R. Tu, J. Cao, Q. Wang, H. Daia, Electrical contacts to carbon nanotubes down to 1 nm in diameter, Appl. Phys. Lett. 87 (2005) 173101.

[33] H.B. Pan, C.M. Wai, Sonochemical one-pot synthesis of carbon nanotube-supported rhodium nanoparticles for room-temperature hydrogenation of arenes, J. Phys. Chem. C 113 (2009) 19782–19788.

ACCEPTED MANUSCRIPT

[34] W. Li, X.-M. Lu, G.-Q. Li, J.-J. Ma, P.-Y. Zeng, J.-F. Chen, et al., First-principle study of SO_2 molecule adsorption on Ni-doped vacancy-defected single-walled (8,0) carbon nanotubes, Appl. Surf. Sci. 364 (2016) 560–566

[35] Q. Zhou, Z. Fu, C. Wang, Y. Tang, H. Zhang, L. Yuan, et al., A DFT study of electronic and magnetic properties of titanium decorating point-defective graphene, Appl. Surf. Sci. 356 (2015) 1025–1031.

[36] R.E. Ambrusi, C.R. Luna, A. Juan, M.E. Pronsato, DFT study of Rh-decorated pristine, B-doped and vacancy defected graphene for hydrogen adsorption, RSC Adv. 6 (2016) 83926-83941.

[37] G. Kresse, D. Joubert, From ultrasoft pseudo-potentials to the projector augmented wave method, Phys. Rev. B 59 (1999) 1758-1775.

[38] G. Kresse, J. Hafner, Ab initio molecular dynamics for liquid metals, Phys. Rev. B 47 (1993) 558-561.

[39] J.P. Perdew, K. Burke, M. Ernzerhof, Generalized gradient approximation made simple, Phys. Rev. Lett. 77 (1996) 3865-3868.

[40] J.P. Perdew, K. Burke, M. Ernzerhof, Erratum: Generalized gradient approximation made simple. Phys. Rev. Lett. 78 (1997) 1396-1396.

[41] H.J. Monkhorst, J.D. Pack, Special points for Brillouin-zone integrations, Phys. Rev. B 13 (1976) 5188-5192.

[42] Y.S. Al-Hamdani, D. Alfe, A. Michaelides, How strongly do hydrogen and water molecules stick to carbon nanomaterials?, J. Phys. Chem. 146 (2017) 094701 1-10.

[43] S. Grimme, Semiempirical gga-type density functional constructed with a long-range dispersion correction, J. Comp. Chem. 27 (2006) 1787-1799.

[44] R. F. W. Bader, Atoms in Molecules: A Quantum Theory, Oxford university Press, New York 1994.

[45] J. Rossato, R.J. Baierle, A. Fazzio, R. Motta, Vacancy formation process in carbon nanotubes: first-principles approach, Nano Lett. 5 (2005) 197-2000.

[46] D.S. Mainardi, P.B. Balbuena, Hydrogen and oxygen adsorption on Rh_n (n = 1−6) clusters, Phys. Chem. A 107 (2003) 10370–10380.

[47] R.V. Reddy, S.K. Nayak, S.N. Khanna, B.K. Rao, P. Jena, Electronic structure and magnetism of Rh_n (n=2–13) clusters, Phys. Rev. B 59 (1999) 5214-5522.

ACCEPTED MANUSCRIPT

[48] K. Saroj, S.E. Nayak, P. Weber, K. Jena, R. Wildberger, P.H. Zeller, et al., Relationship between magnetism, topology, and reactivity of Rh clusters, Phys. Rev. B 56 (1997) 8849-8854.

[49] F. Aguilera-Granja, J.L. Rodríguez-López, K. Michaelian, E.O. Berlanga-Ramírez, A. Vega, Structure and magnetism of small rhodium clusters, Phys. Rev. B 66 (2002) 224410.

[50] D.L. Cocke, K.A. Gingerich, Thermodynamic investigation of the gaseous molecules TiRh, Rh_2, and Ti_2Rh by mass spectrometry, J. Chem. Phys. 60 (1974) 1958-1965.

[51] K. Balasubramanian, D. Liao, Spectroscopic properties of low-lying electronic states of rhodium dimer, J. Phys. Chem. 93 (1989) 3989-3992.

[52] T. Nongnual, J. Limtrakul, Healing of a vacancy defect in a single-walled carbon nanotube by carbon monoxide disproportionation, J. Phys. Chem. C 115 (2011) 4649–4655.

[53] Y. Ma, P.O. Lehtinen, A.S. Foster, R.M. Nieminen, Magnetic properties of vacancies in graphene and single-walled carbon nanotubes, New J. Phys. 6 (2004) 1-16.

[54] M.G. Mashapa, N. Chetty, S.S. Ray, Ab initio studies of vacancies in (8,0) and (8,8) single-walled carbon and boron nitride nanotubes, J. Nanosci. Nanotechnol. 12 (2012) 7030–7036.

[55] A. Barinov, O. Bariş Malcioğlu, S. Fabris, T. Sun, L. Gregoratti, M. Dalmiglio, M. Kiskinova et al., Initial stages of oxidation on graphitic surfaces: photoemission study and density functional theory calculations, J. Phys. Chem. C 113 (2009) 9009-9013.

[56] M. Park, B-H. Kim, S. Kim, D-S. Han, G. Kim, K-R. Lee, Improved binding between copper and carbon nanotubes in a composite using oxygen-containing functional groups, Carbon 49 (2011) 811-818.

[57] B.R. Sathe, B.A. Kakade, A. Kushwaha, M. Aslam, V.K. Pillai, Synthesis of Rh–carbon nanotube based heterostructures and their enhanced field emission characteristics, Chem. Commun. 46 (2010) 5671-5673.

ACCEPTED MANUSCRIPT

Figure Captions

Figure 1. Optimized geometries of a single C vacancy in (8,0) SWCNT: -a perpendicular vacancy configuration and -b parallel vacancy configuration. Total DOS curves for -c perpendicular vacancy configuration and -d parallel vacancy configuration. The dotted line indicates the Fermi level.

Figure 2. Charge transfer among the C atoms of the SWCNT containing a single vacancy (perpendicular configuration). Red and blue indicate the atom that gains (negative charge) and loses (positive charge) electrons, respectively. The bar on the left is in e^- unit.

Figure 3. Optimized atomic structures of (8,0) SWCNT containing a reconstructed single vacancy when a O_2 molecule is adsorbed.

Figure 4. Density of states for O_2 adsorption on defective SWCNT. -a Total DOS curve. -b PDOS for the *p*-states of oxygen atoms (the blue line corresponds to the isolated O_2 molecule and the red line corresponds to adsorbed O atoms). -c PDOS curves for the *p*-states of C atoms. The PDOS curves of *s*-states are not shown because these states practically do not contribute to Total DOS curve. The dotted line indicates the Fermi level.

Figure 5. Charge transfer between C and O atoms of the SWCNT containing a single vacancy. Red and blue indicate that the atom gains (negative charge) and loses (positive charge) electrons respectively. The bar on the left is in e^- unit.

Figure 6. Optimized structure of Rh_n adsorption on defective SWCNT without (-a to -d) and with (-e to -h) adsorbed O_2.

Figure 7. Total and projected density of states for Rh_n adsorption on defective SWCNT and oxygented vacancy. -a and -b atomic Rh,-c and -d Rh_2 dimer, -e and -f Rh_3, -g and -h Rh_4. The dotted line indicates the Fermi level.

Figure 8. Charge transfer for Rh_n adsorption on defective SWCNT: -a to -d without and -e to -h with O_2 adsorbed. The red and blue colors indicate that the atom gains (negative charge) and loses (positive charge) electrons respectively. The bar on the top is in e^- unit.

ACCEPTED MANUSCRIPT

Figure Lists

Figure 1.

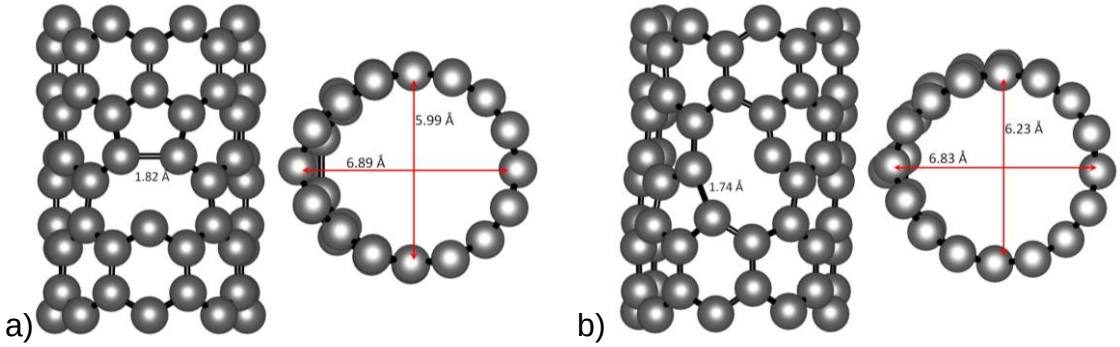

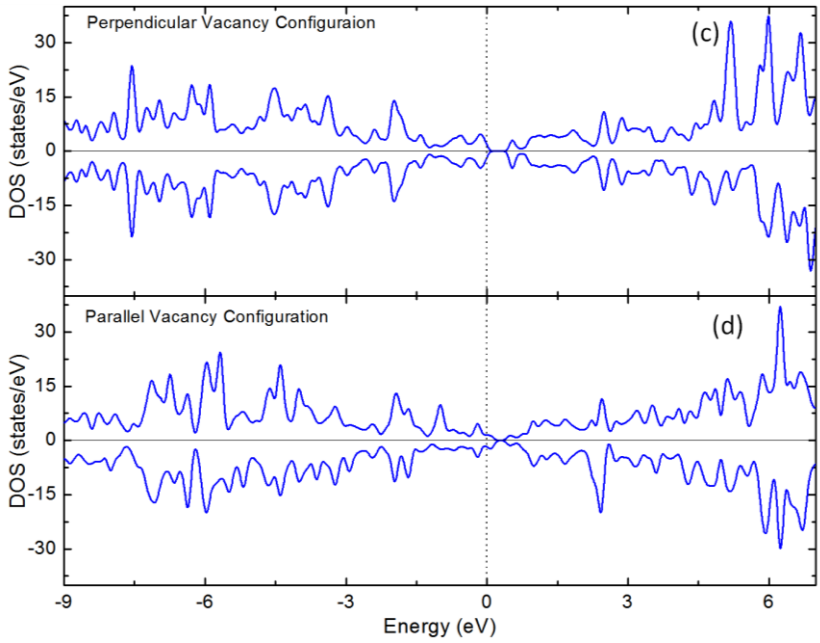

ACCEPTED MANUSCRIPT

Figure 2.

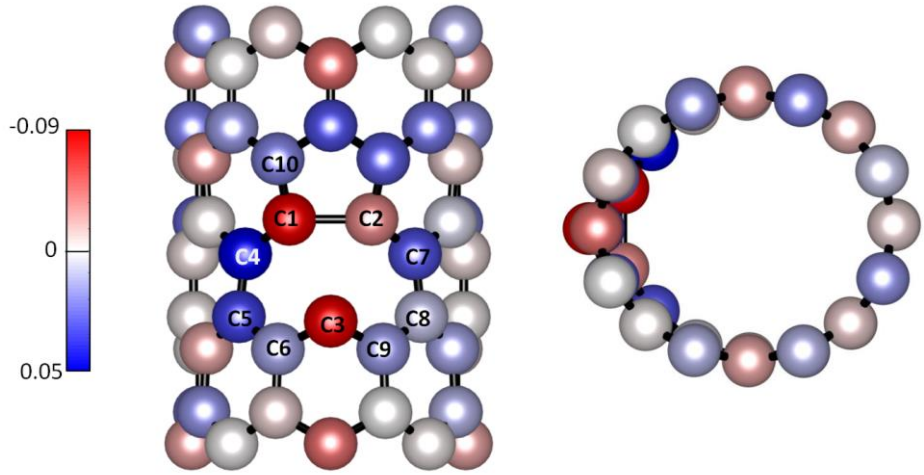

ACCEPTED MANUSCRIPT

Figure 3.

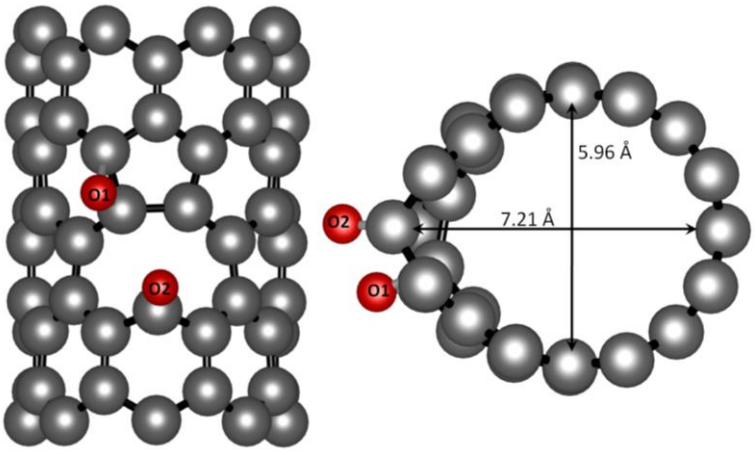

ACCEPTED MANUSCRIPT

Figure 4.

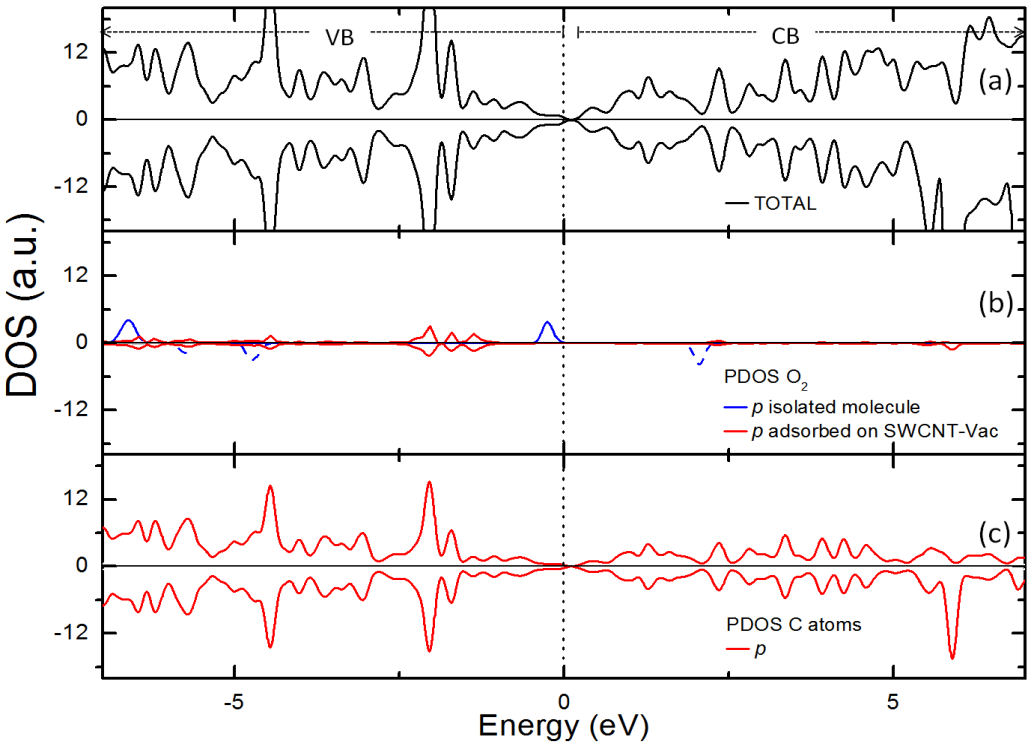

ACCEPTED MANUSCRIPT

Figure 5.

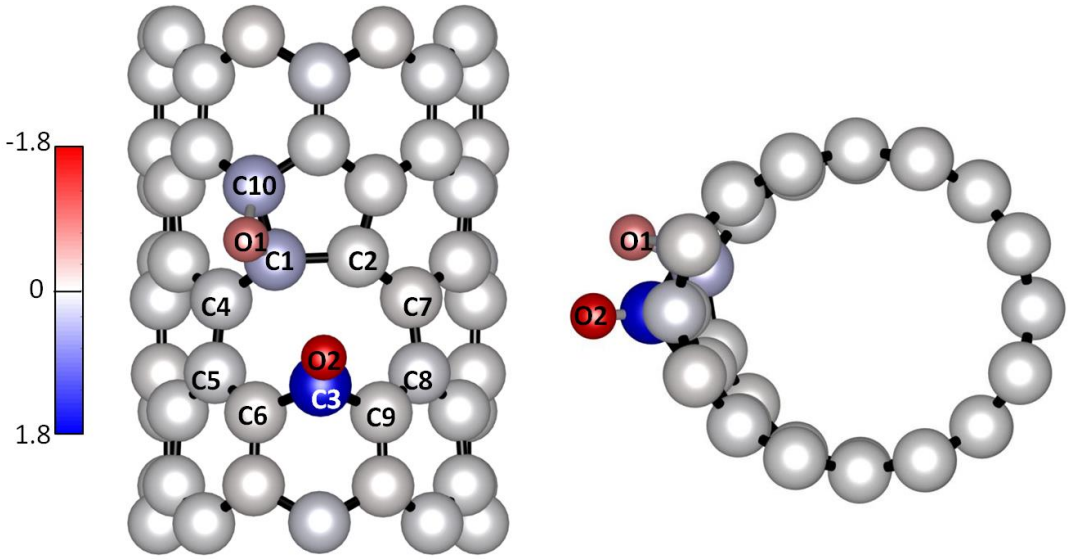

ACCEPTED MANUSCRIPT

Figure 6.

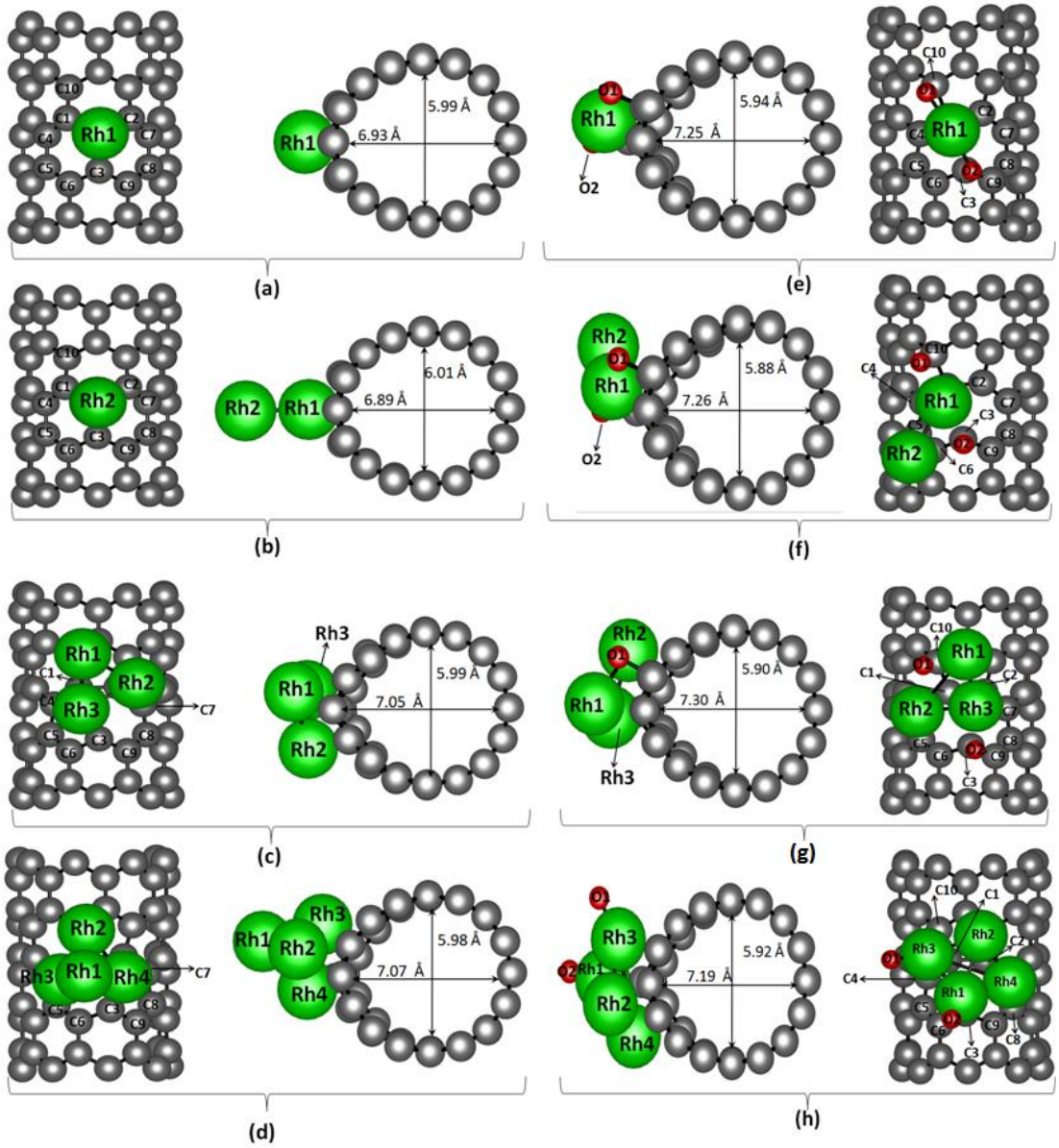

ACCEPTED MANUSCRIPT

Figure 7.

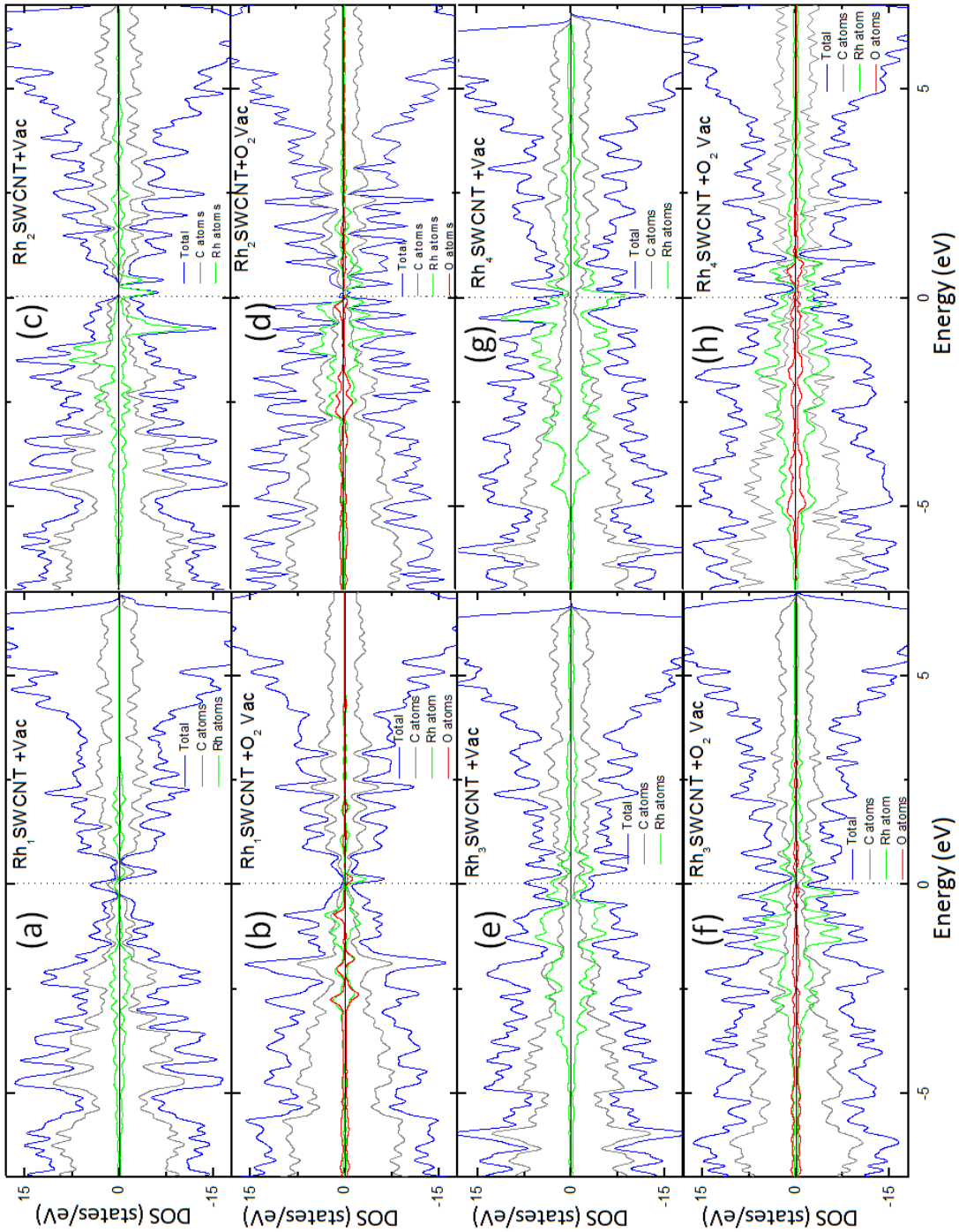

ACCEPTED MANUSCRIPT

Figure 8.

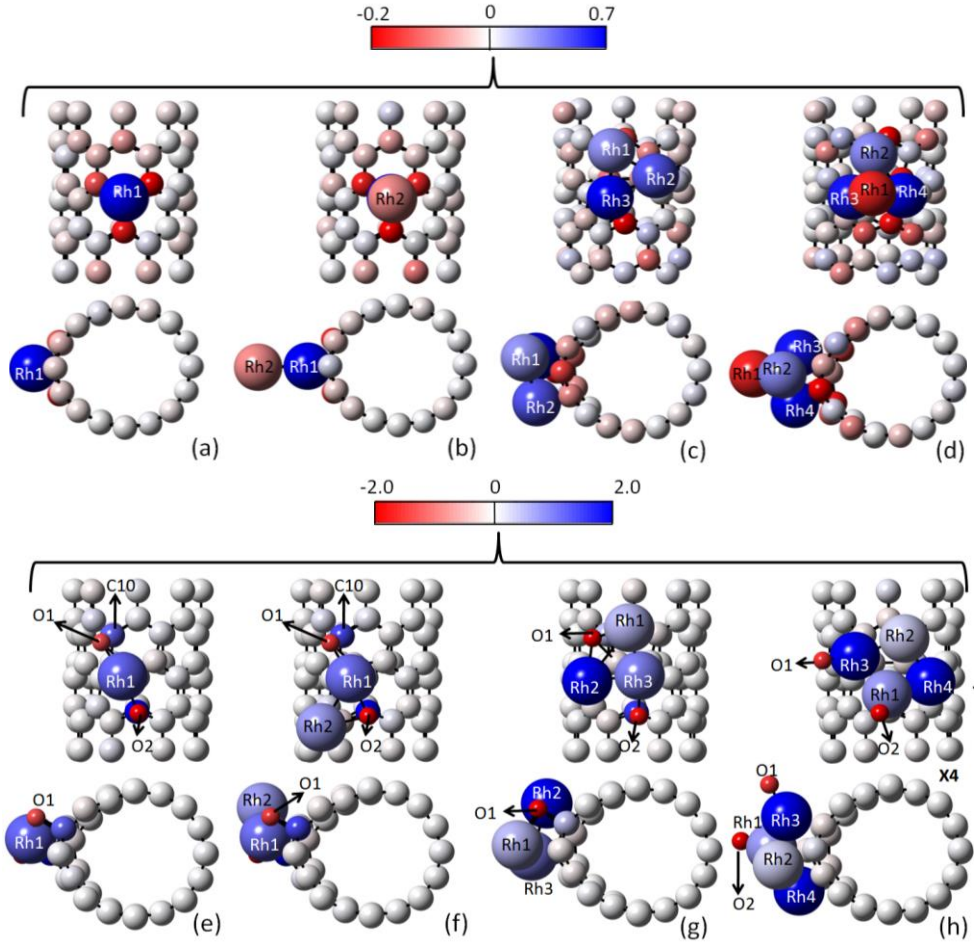

ACCEPTED MANUSCRIPT

Table Lists

Table 1. Geometry, binding energies (E_b) per atom, magnetic moment (μ), bond lengths (d_{Rh-Rh}) and angles, for isolated Rh_n (n = 1-4) clusters.

System	Geometry	E_b/atom (eV)	μ(μB)	d_{Rh-Rh} (Å)	Angles (º)
Rh_1	-	-	2.1	-	-
Rh_2	linear	-1.89	4.0	2.21	-
Rh_3	triangular	-2.54	3.0	All bonds 2.38	All angles 60
Rh_4	tetrahedral	-3.01	0.0	All bonds 2.45	All angles 60

ACCEPTED MANUSCRIPT

Table 2. Band gap (E_g), magnetic moment (μ), work function (WF) and formation energy (E_{form}) for defective (8,0) SWCNT.

Vacancy configuration	class	E_g (eV)	μ (μ_B)	WF (eV)	E_{form} (eV)
Perpendicular	semiconductor	0.48	0.0	4.89	5.88
Parallel	metal	-	1.0	4.72	6.65

ACCEPTED MANUSCRIPT

Table 3. Geometry, bond length and angles for both functional groups obtained after O_2 adsorption on defective (8,0) SWCNT

Group	Geometry	d_{O-C} (Å)	d_{C-C}(Å)	Angle (º)
C - O - C	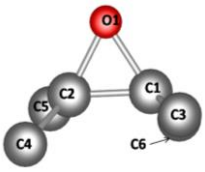	O-C1: 1.46 O-C2: 1.47	C1-C2: 1.48 C1-C3: 1.50 C1-C6: 1.59 C2-C4: 1.49 C2-C5: 1.47	C1 - O - C2: 60.7 O - C2- C1: 60.2
C = O	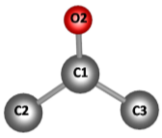	O-C1: 1.22	C1-C2: 1.51 C1-C2: 1.52	C2-C1-O: 126.2º C3-C1-O: 127.8 º

ACCEPTED MANUSCRIPT

Table 4. Bond distances for Rh_n adsorbed on SWCNT containing a single vacancy without and with oxygen, SWCNT+Vac and SWCNT+O_2 Vac respectively.

	SWCNT+Vac			SWCNT+O_2 Vac				
	d_{C-C}(Å)	d_{Rh-C}(Å)	d_{Rh-Rh}(Å)	d_{C-C}(Å)	d_{Rh-C}(Å)	d_{Rh-Rh}(Å)	d_{O-C}(Å)	d_{O-Rh}(Å)
Rh	C1-C10:1.39 C1-C4/C7-C2:1.42 C4-C5/C6-C3/C8-C7:1.43 C5-C6/C9-C8:1.44 C1-C2:2.64	Rh-C1:1.86 Rh-C2:1.95 Rh-C3:1.95	-	C4-C5/C9-C8/C8-C7:1.41 C5-C6:1.43 C7-C2:1.45 C1-C4/C6-C3:1.50 C1-C2/C3-C9:1.52 C1-C10:1.55	Rh-C1:2.01 Rh-C3:2.10 Rh-C2:2.77	-	O2-C3: 1.32 O1-C10:1.43 O1-C1:2.26	Rh-O1:1.96 Rh-O2:2.00
Rh_2	C1-C10:1.40 C1-C4/C7-C2:1.42 C4-C5/C8-C7:1.43 C5-C6/C6-C3/C9-C8:1.44 C1-C2:2.65	Rh1-C3:1.85 Rh1-C2:1.96 Rh1-C1:1.97	2.46	C4-C5/C9-C8:1.40 C8-C7:1.42 C5-C6/C7-C2:1.45 C1-C4/C3-C9:1.49 C1-C2/C6-C3:1.51 C1-C10:1.55	Rh1-C1/Rh2-C6:2.07 Rh1-C10:2.60 Rh1-C2:2.85	2.79	O2-C3: 1.35 O1-C10:1.43 O1-C1:2.27	Rh1-O1:2.01 Rh1-O2:2.07 Rh2-O2:2.31
Rh_3	C1-C10:1.40 C1-C4/C7-C2:1.42 C4-C5/C8-C7:1.43 C5-C6/C6-C3/C9-C8:1.44 C1-C2:2.65	Rh3-C3: 1.87 Rh2-C2:2.06 Rh1-C10:2.17	Rh1-Rh3:2.57 Rh2-Rh3:2.58 Rh1-Rh2: 2.67	C9-C8:1.40 C4-C5/C5-C6/C8-C7:1.43 C1-C4/C3-C9/C7-C2:1.48 C1-C2/C1-C10/C6-C3:1.53	Rh3-C4: 2.05 Rh2-C4:2.11 Rh1-C10:2.52	Rh1-Rh3:2.49 Rh2-Rh3:2.60 Rh1-Rh2: 3.56	O2-C3: 1.32 O1-C10:1.50 O1-C1:2.39	Rh3-O2:2.03 Rh1-O1:2.06 Rh2-O1:2.16
Rh_4	C8-C7:1.41 C3-C9/C9-C8:1.43 C4-C5:1.44 C1-C4/C5-C6/C6-C3:1.46 C1-C10:1.48 C1-C2:1.58	Rh4-C3:1.88 Rh2-C10:2.10 Rh3-C1:2.13 Rh3-C4/Rh4-C2:2.18	Rh1-Rh3:2.47 Rh1-Rh2: 2.49 Rh1-Rh4:2.57 Rh3-Rh4:2.59 Rh2-Rh3:2.62 Rh2-Rh4:2.67	C4-C5:1.41 C5-C6/C8-C7/C9-C8:1.43 C1-C10:1.45 C1-C2:1.57	Rh1-C3:1.89 Rh4-C7:2.10 Rh2-C10:2.17 Rh3-C1:2.19 Rh2-C2:2.67	Rh1-Rh3/Rh1-Rh4:2.52 Rh2-Rh3:2.54 Rh2-Rh4:2.64 Rh1-Rh2: 2.88 Rh3-Rh4:3.85	O2-C3: 3.16 O1-C10:3.47 O1-C1:3.67	Rh1-O2:1.74 Rh3-O1:1.75

ACCEPTED MANUSCRIPT

Table 5. Binding energy (E_b), magnetic moment (μ) and work function (WF) for Rh_n cluster adsorbed on SWCNT containing a single vacancy (SWCNT+Vac) and this defect with O_2 adsorbed (SWCNT+O_2Vac).

Rh_n Adsorption	**SWCNT + Vac**			**SWCNT + O_2 Vac**		
	E_b(eV)	**μ (μ_B)**	**WF (eV)**	**E_b(eV)**	**μ (μ_B)**	**WF (eV)**
Rh	7.56	1.0	4.26	5.12	1.0	4.75
Rh_2	6.31	2.0	4.46	4.92	2.0	4.56
Rh_3	4.11	2.1	4.16	5.14	1.0	4.33
Rh_4	3.63	2.0	4.24	4.59	2.2	5.09